

Corrigendum

Corrections to the ‘Enhancement of microwave tomography through the use of electrically conducting enclosures’

C Gilmore and J LoVetri 2008 *Inverse Problems* 24 035008

In a previous paper [1] we considered the problem of performing microwave tomography (MWT) inside of conducting enclosures. We presented several examples comparing enclosed-region inversions directly with open-region inversions. The results presented therein were produced with a code containing two errors. These errors are as follows.

- (i) In both the enclosed-region and open-region inverse solvers, the computation of the multiplicative regularizer (MR) was incorrectly implemented. This error involved the method of calculating the derivatives associated with the MR term, and was identical for both solvers.
- (ii) In the *open-region* forward solver only, an error was made in the computation of the adjoint operator used to generate the search direction for the CG-FFT algorithm. Thus, the data that were generated for the open-region problem, and used by the inverse solver, were incorrect. This error degraded the imaging results in a significant way only in the open-region examples with high-contrast scatterers.

These errors have been corrected and the computational examples in [1] re-generated. The corrected results are shown in figures 1–5, which replace figures 3–7 in the original paper. The corrected p -norms of the reconstruction error are presented in table 1.

The first error does not change the comparison of enclosed and open-region inversions shown in [1], as it affected the two problems (open/enclosed) in the same way. However, as it adversely affected the open-region reconstructions only, the second error caused the enhanced performance of the enclosed-region inversions observed in two of the examples: the square scatterer (figure 1, figure 3 in [1]) and multi-frequency concentric squares (figure 4, figure 6 in [1]). Thus, the examples considered therein no longer support the statement that we have several examples ‘in which the use of a PEC cylinder to surround the scattering object improved the inversion results over the usual method of embedding the scatterer in an infinite background medium’. The reconstructions of these particular examples are now much more similar. We note that these corrected results offer support to the conclusions in [2], where it is shown that the linear enclosed operator offers a somewhat different ‘quality’ of information content than the open-region linear operator, but does not offer any more ‘quantity’ of information. This does leave open the question of whether the information is independent information about the scatterer.

While these examples show similar reconstructions for the enclosed/open-region systems, we note that for some internal areas of the scatterers, improvements are visible in the enclosed reconstructions. For example, in both the low- and mid-contrast concentric squares (figures 2 and 3), the value of the complex permittivity of the internal square is reconstructed more accurately inside the conducting enclosure. This is best seen in the 1D plots of both figures (sub-figure d).

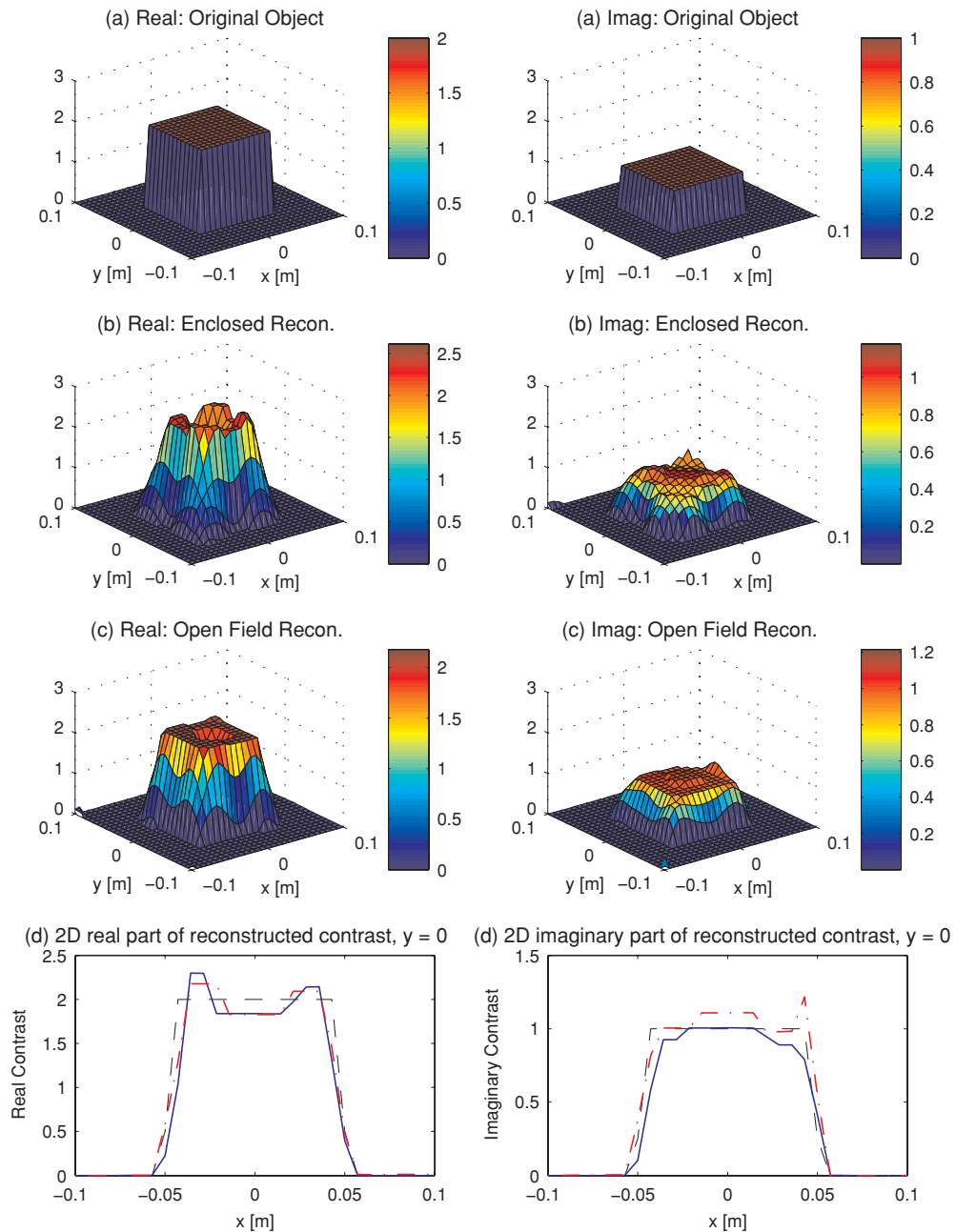


Figure 1. Square scatterer reconstruction after 1024 steps of the MR-CSI algorithm. (a) The exact contrast of the scatterer. (b) The MR-CSI reconstruction when both the forward data generation and inversion include a cylindrical PEC shield. (c) Reconstruction when both the forward data generation and inversion assume a free-space background. (d) A 2D cross section at $y = 0$ for (black dash line) exact, (blue solid line) enclosed reconstruction and (red dash-dot) free-space reconstruction.

(This figure is in colour only in the electronic version)

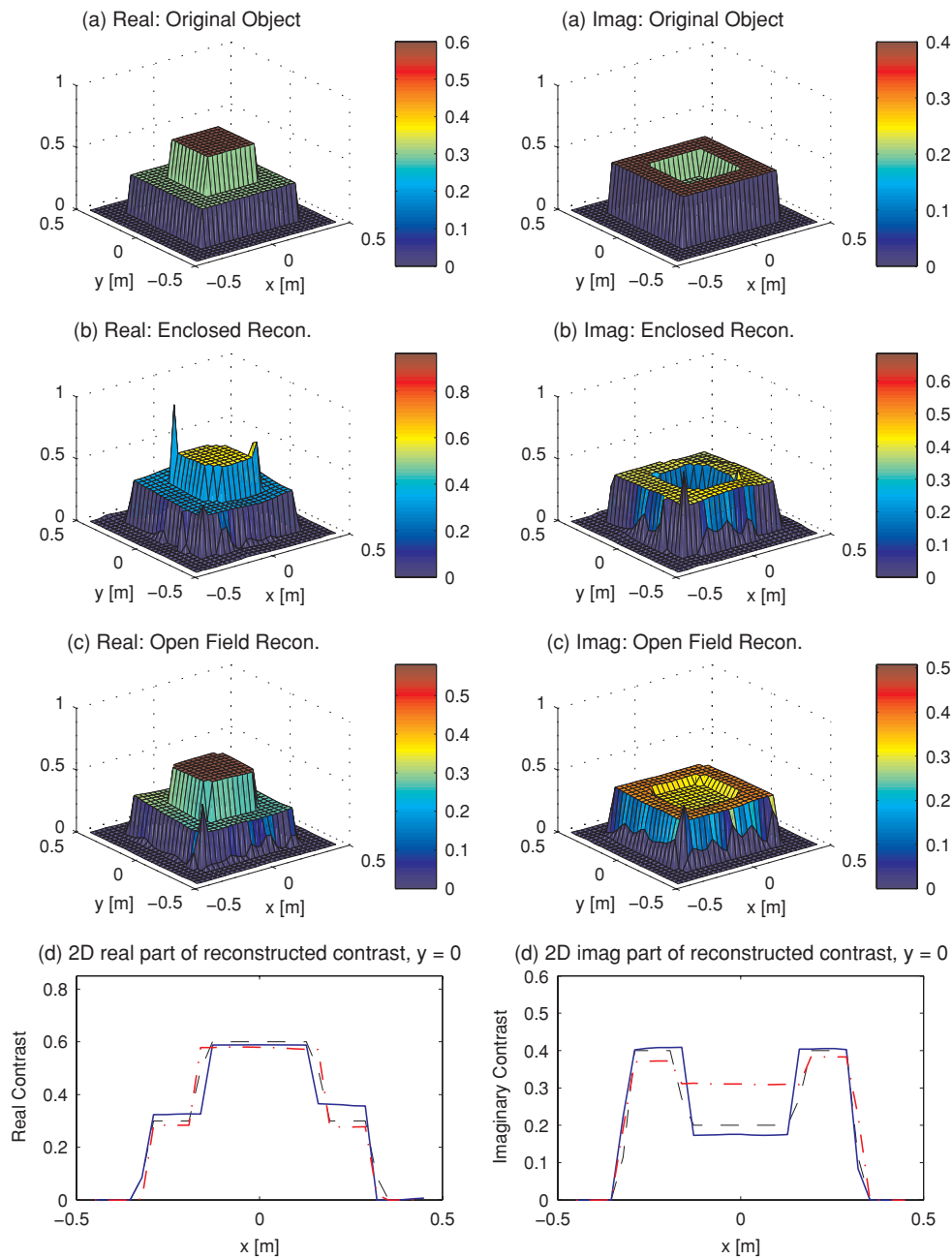


Figure 2. Low-contrast concentric squares after 1024 steps of the MR-CSI algorithm. (a) The exact contrast of the scatterer. (b) The MR-CSI reconstruction when both the forward data generation and inversion include a cylindrical PEC shield. (c) Reconstruction when both the forward data generation and inversion assume a free-space background. (d) A 2D cross section at $y = 0$ for (black dash line) exact, (blue solid line) enclosed reconstruction and (red dash-dot) free-space reconstruction.

(This figure is in colour only in the electronic version)

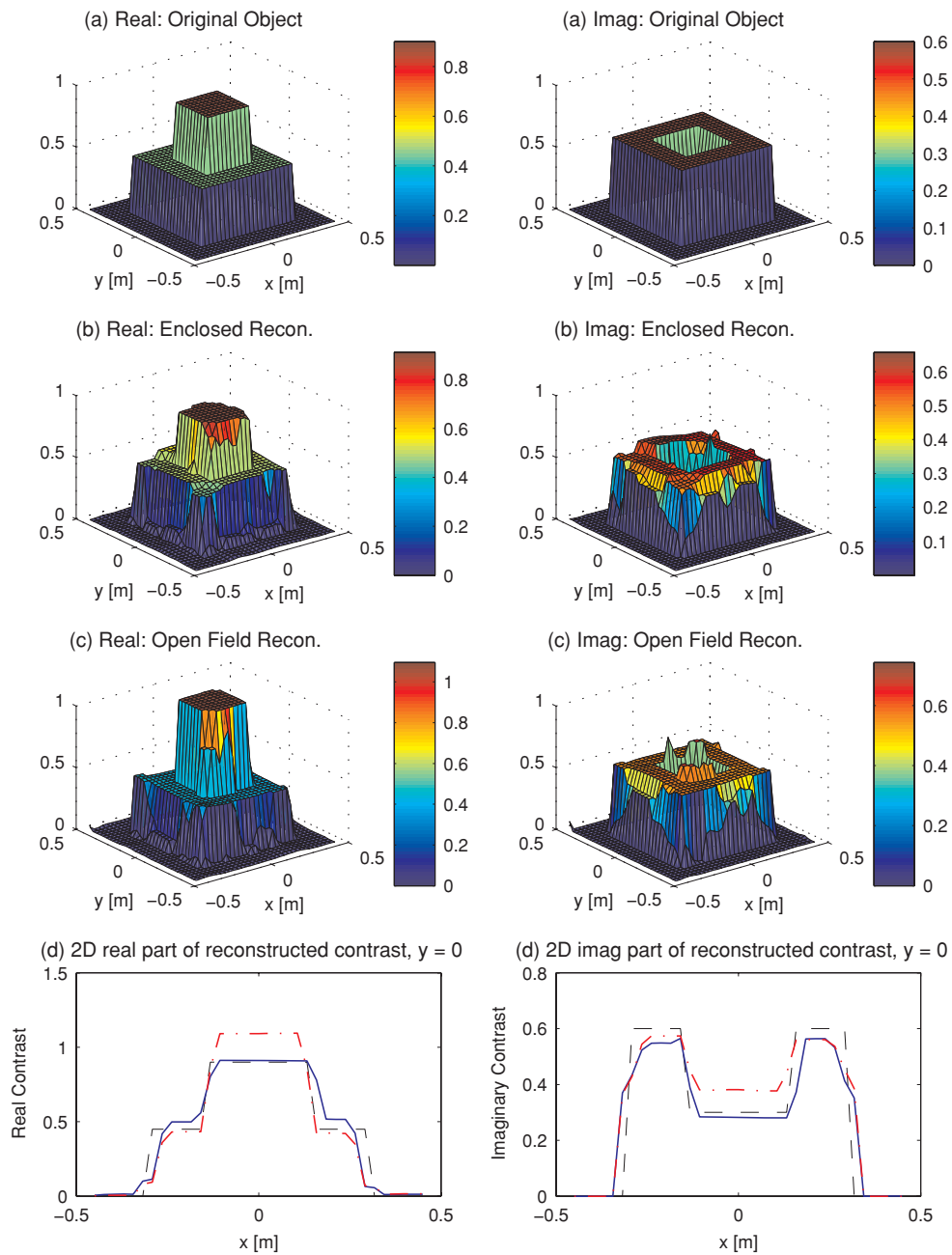


Figure 3. Mid-contrast concentric squares after 1024 steps of the MR-CSI algorithm. (a) The exact contrast of the scatterer. (b) The MR-CSI reconstruction when both the forward data generation and inversion include a cylindrical PEC shield. (c) Reconstruction when both the forward data generation and inversion assume a free-space background. (d) A 2D cross section at $y = 0$ for (black dash line) exact, (blue solid line) enclosed reconstruction, and (red dash-dot) free-space reconstruction.

(This figure is in colour only in the electronic version)

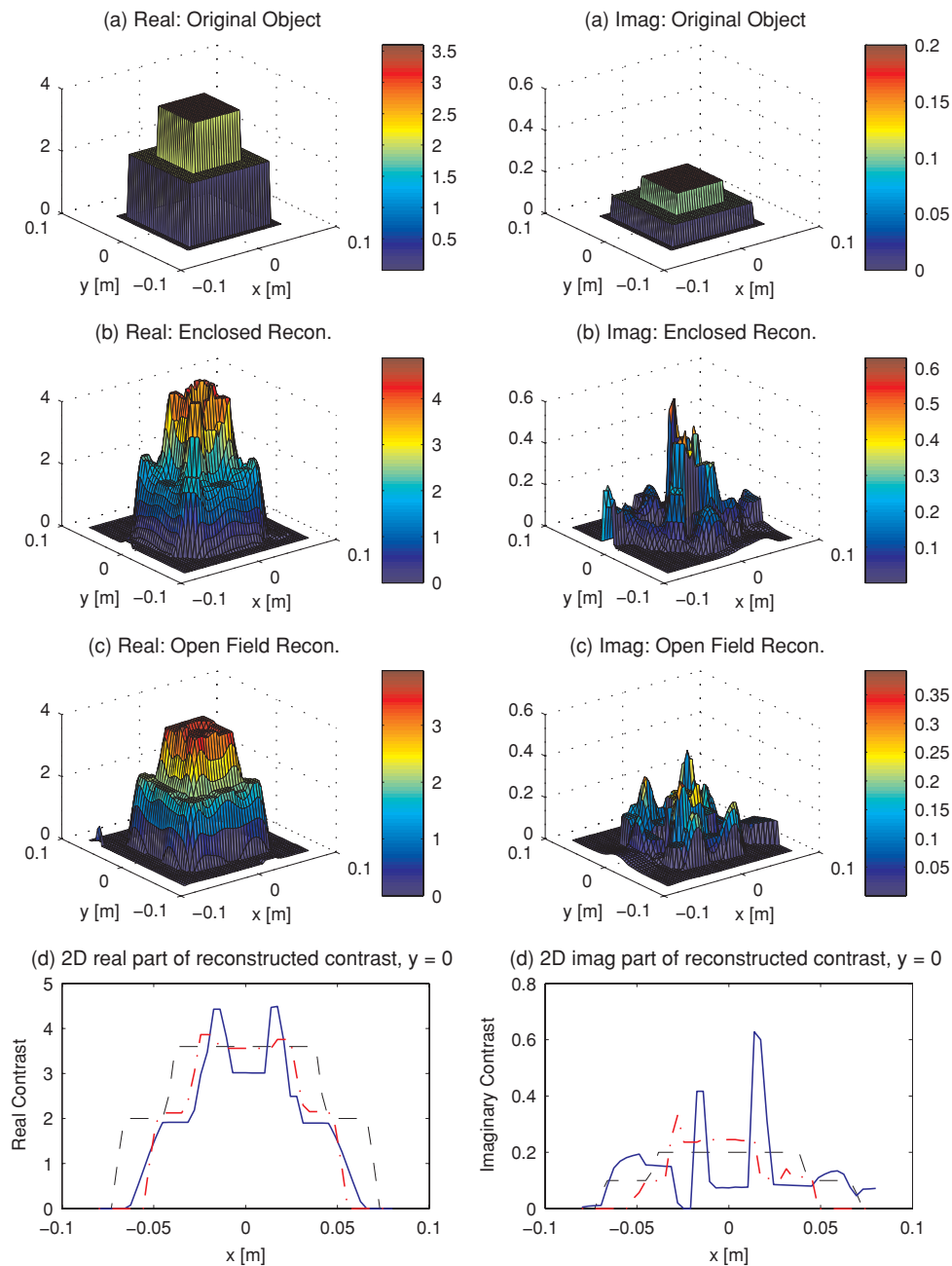


Figure 4. Multi-frequency concentric squares after 1024 steps of the MR-CSI algorithm. (a) The exact contrast of the scatterer. (b) The MR-CSI reconstruction when both the forward data generation and inversion include a cylindrical PEC shield. (c) Reconstruction when both the forward data generation and inversion assume a free-space background. (d) A 2D cross section at $y = 0$ for (black dash line) exact, (blue solid line) enclosed reconstruction and (red dash-dot) free-space reconstruction.

(This figure is in colour only in the electronic version)

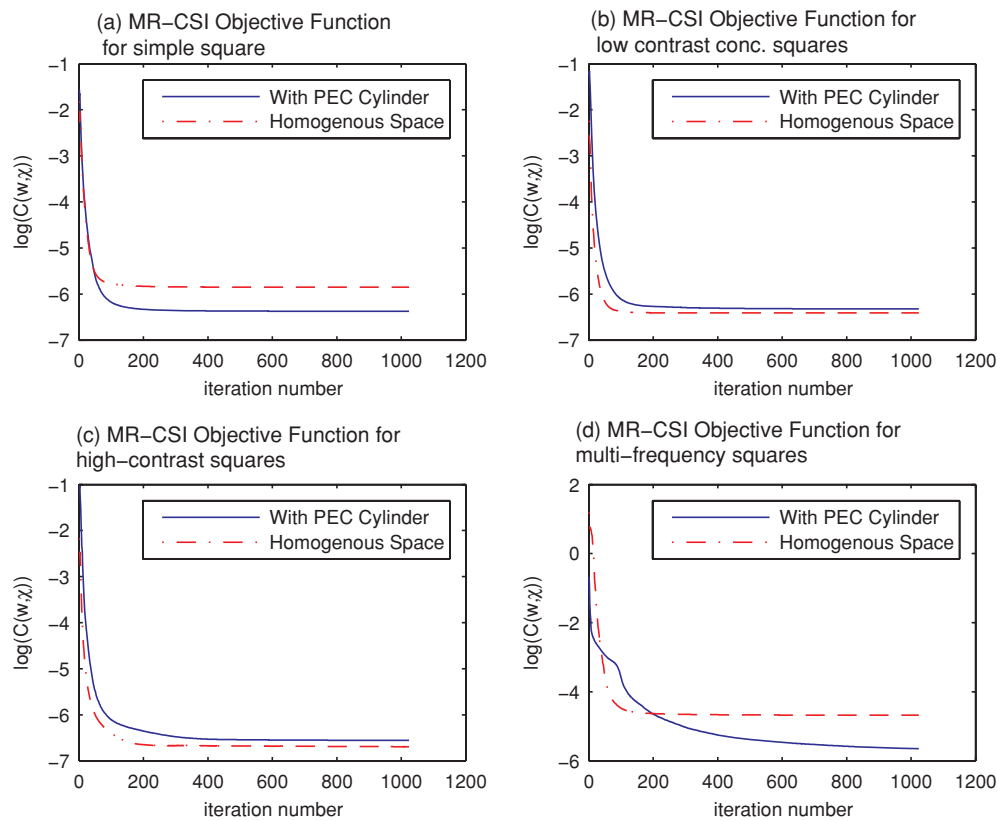


Figure 5. The MR-CSI objective function, $C(w, \chi)$ versus iteration number for (a) simple square, (b) low-contrast concentric squares, (c) high-contrast concentric squares and (d) multi-frequency concentric squares reconstruction.

(This figure is in colour only in the electronic version)

We believe that there can be significant advantages to the use of the enclosed region MWT. Practical advantages arising from the use of an enclosed system include more accurate system modeling, shielding from outside noise and a better signal-to-noise ratio [2]. The theoretical advantages, such as the possibility of obtaining independent information via the use of both types of system, will be discussed in a future publication. Preliminary microwave tomographic results, based on synthetic data, obtained using conducting enclosures of arbitrary shapes have been presented in [3] and some of the potential theoretical advantages of using such systems were also discussed therein.

Table 1. Relative vector norms of reconstructed contrast functions.

	Reconstruction with PEC enclosure	Reconstruction without PEC enclosure
Simple squares (figure 1)		
L_1 error	27.3%	18.3%
L_2 error	26.5%	19.4%
L_∞ error	63.2%	75.3%
Low-contrast concentric squares (figure 2)		
L_1 error	15.4%	16.1%
L_2 error	17.8%	17.1%
L_∞ error	72.0%	56.4%
High-contrast concentric squares (figure 3)		
L_1 error	20.0%	19.9%
L_2 error	22.3%	22.0%
L_∞ error	53.3%	48.0%
Multi-frequency concentric squares (figure 4)		
L_1 error	48.8%	45.8%
L_2 error	51.9%	51.8%
L_∞ error	55.5%	55.5%

References

- [1] Gilmore C and LoVetri J 2008 Enhancement of microwave tomography through the use of electrically conducting enclosures *Inverse Problems* **24** 035008
- [2] Crocco L and Litman A 2009 On embedded microwave imaging systems: retrievable information and design guidelines *Inverse Problems* **25** 065001
- [3] Mojabi P, Gilmore C, Zakaria A and LoVetri J 2009 Biomedical microwave inversion in conducting cylinders of arbitrary shapes *13th Int. Symp. on Antenna Technology and Applied Electromagnetics and the Canadian Radio Science Meeting, ANTEM/URSI 2009* pp 1–4